Journal of Basics and Applied Sciences Research (JOBASR)
ISSN (print): 3026-9091, ISSN (online): 1597-9962
Volume 3(4) July 2025
DOI: https://dx.doi.org/10.4314/jobasr.v3i4.9

Sensitivity Analysis and Applications of Laplace Adomian Decomposition Method In Solving Fractional –Order Malaria Model

Agbata, B.C.[1*], Atabo, O .V[2], Senewo, E.O[3], Micheal B.D[4], Ezugorie I.G[5], & Ahman, Q.O[6]

[1,2,3,4 &6]Department of Mathematics and Statistics, Faculty of Science, Confluence University of Science and Technology, Osara, Nigeria.
[5]Department of Industrial/ Applied Statistics , Enugu State University of Science and Technology, Enugu, Nigeria
[*]Corresponding Author Email: abcinfotech08@gmail.com

ABSTRACT
This study explores the sensitivity analysis and implementation of the Laplace-Adomian Decomposition Method (LADM) in solving a fractional-order malaria transmission model utilizing the Caputo fractional derivative. A deterministic compartmental model comprising eight ordinary differential equations is formulated to capture the dynamics of malaria spread. Key mathematical properties of the model, including the positivity of solutions and the existence of an invariant region, are rigorously examined. Stability analysis reveals that the disease-free equilibrium remains locally stable when the basic reproduction number is less than one, based on the next-generation matrix approach. To approximate solutions of the fractional-order system, LADM is employed, generating a rapidly converging infinite series under appropriate conditions. Parameter values are estimated using MATLAB's *fmincon* optimization algorithm, calibrated with empirical malaria data extracted from published sources. LADM integrates the Laplace transform with the Adomian Decomposition Method by first applying the Laplace transform, breaking down nonlinear terms via Adomian polynomials, and finally applying the inverse Laplace transform to derive the solution. The study successfully applies LADM to obtain approximate solutions for the malaria model and reaffirms that the disease-free equilibrium is stable when the reproduction number falls below one. Findings also show that enhancing treatment efficacy within the human population leads to a marked decline in malaria prevalence. Sensitivity analysis identifies key parameters that influence disease transmission, highlighting that reducing contact between susceptible individuals and infectious mosquitoes, alongside prompt treatment of infected individuals, is vital for disease control. Unlike previous models based solely on classical ADM, this work integrates the Laplace transform to improve both convergence speed and solution accuracy. Moreover, real malaria data from Nigeria is incorporated to ensure practical relevance and accuracy of the model.

Keywords:
Laplace-Adomian Decomposition, Malaria/Tuberculosis (TB) co-infection, Fractional-order model, Mathematical modelling, Data fitting

INTRODUCTION

Malaria continues to pose a major public health threat, particularly in tropical and subtropical regions where Anopheles mosquitoes—its primary vectors—are widespread.

The World Health Organization (WHO, 2023) reported approximately 247 million malaria cases worldwide in 2021, with nearly 95% occurring in Sub-Saharan Africa. The disease is caused by Plasmodium parasites, with *Plasmodium falciparum* recognized as the deadliest species.

How to cite this article: Agbata, B.C, Atabo, O .V, Senewo, E.O, Micheal B.D, Ezugorie I.G. and Ahman, Q.O (2025). Sensitivity Analysis and Applications of Laplace Adomian Decomposition Method in Solving Fractional –Order Malaria Model. *Journal of Basics and Applied Sciences Research*, *3*(4), 73-89. https://dx.doi.org/10.4314/jobasr.v3i4.9

Transmission occurs via infected mosquito bites, meaning environmental conditions and socio-economic circumstances play a significant role in influencing malaria distribution and prevalence (Bhatt et al, 2022; Cator et al, 2023; Ghosh et al, 2022). Mathematical modeling has been vital for understanding malaria transmission patterns. Compartmental models, in particular, have provided frameworks to represent the interactions between human and mosquito populations (Chitnis et al, 2008). These models help simulate transmission under different scenarios, allowing researchers to evaluate control measures such as insecticide-treated nets (ITNs) and antimalarial drugs (Reiner et al, 2023). Despite notable advancements, malaria control continues to face significant obstacles, including the emergence of drug-resistant *Plasmodium falciparum* strains in Southeast Asia and parts of Africa, underscoring the need for new treatments and vigilant surveillance (Ashley et al., 2023). In addition, resistance to pyrethroid insecticides used in ITNs and indoor residual spraying (IRS) has weakened vector control efforts (Hemingway et al, 2022). Climate change also threatens to shift malaria transmission zones by expanding mosquito habitats, further complicating eradication strategies (Ryan et al, 2023). In this context, mathematical models have become indispensable for forecasting transmission patterns and designing adaptive public health interventions.

Recent advancements in modeling have introduced greater complexity, including the use of fractional-order differential equations, which offer a refined framework for incorporating memory-dependent processes in disease dynamics (Diethelm, 2022). Such models more accurately represent real-world malaria transmission by accounting for factors like delayed immunity and uneven exposure across populations (Ngonghala et al, 2021). Sensitivity analysis within these models has been instrumental in pinpointing the most influential parameters such as mosquito biting frequency, recovery rates, and the basic reproduction number ($\mathbb{R}0$) which help determine whether a malaria outbreak will persist or decline (Ndii et al, 2020; Bhattacharya et al, 2023). Simulations have shown that targeted interventions, including timely treatment and effective mosquito control, can drastically reduce infection rates (Yang and Xiao, 2023). Current strategies to combat malaria emphasize both pharmaceutical approaches and vector control. WHO recommendations include broad deployment of ITNs, the use of IRS, and mass administration of antimalarial drugs (WHO, 2023). Recent breakthroughs, such as the RTS,S malaria vaccine, have shown encouraging results in lowering infection rates among children in high-transmission areas (Draper et al, 2022). The impact and efficiency of these interventions are frequently assessed through mathematical modeling, helping decision-makers optimize how resources are allocated and interventions are timed (Winskill et al, 2023; Pamungkas and Eljatin, 2024). Furthermore, models that integrate variables such as climate change and socio-economic conditions provide more comprehensive insights into malaria's persistence and potential resurgence (Parham and Michael, 2022).

MATERIALS AND METHODS

Model Formulation

A deterministic compartmental model has been formulated to analyze the transmission dynamics of malaria. The total human population $N_H(t)$, is divided into five (5) distinct compartments: susceptible humans S_H ,exposed humans to malaria E_M , infected humans with malaria I_M treated humans due to malaria T_M , and recovered humans from malaria R . Likewise, the mosquito vector population is categorized into three (3) compartments: susceptible vectors S_V exposed vectors E_V and infected vectors I_V .Humans are recruited into the susceptible class at a rate denoted by Λ_H , while β_M represents the effective contact rate, incorporating the probability of infection per contact between a susceptible human and a mosquito infected with malaria. The progression rate from the exposed to the infected human class is indicated by θ_M . Recovery from malaria in humans occurs at a rate of α_M . Individuals who have recovered may lose immunity and return to the susceptible class at a rate given by ω_M . The natural death rate of humans is μ_H , and the malaria-induced mortality rate is δ_M . The rate of compliance with treated bed net usage, aimed at reducing malaria transmission, is represented by ϕ , and the mosquito biting rate per unit time is given as m . The recruitment rate of malaria-transmitting *Anopheles* mosquitoes is represented by Λ_V , with β_V being the effective contact rate that includes the probability of mosquito infection per bite from an infected human. Exposed vectors progress to the infected stage at a rate of θ_V . The natural death rate of mosquito vectors is μ_V , while the mortality rate associated with the search for a blood meal is represented by δ_V .

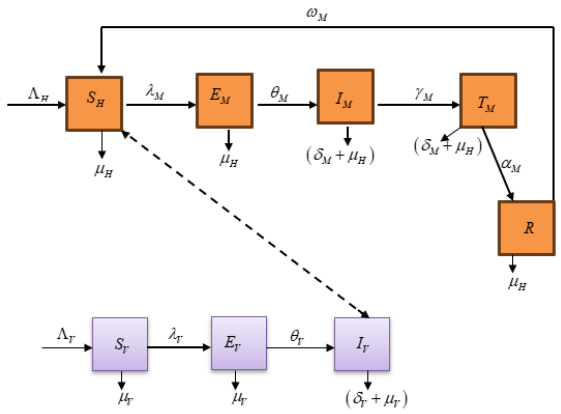

Figure 1: Schematic diagram for the model

The Model equations

The differential equations that describe the above illustrations are.

$$\frac{dS_H}{dt} = \Lambda_H - (\lambda_M + \mu_H) S_H + \omega_M R$$
$$\frac{dE_M}{dt} = \lambda_M S_H - (\theta_M + \mu_H) E_M$$
$$\frac{dI_M}{dt} = \theta_M E_M - (\gamma_M + \delta_M + \mu_H) I_M$$
$$\frac{dT_M}{dt} = \gamma_M I_M - (\alpha_M + \delta_M + \mu_H) T_M \quad (5)$$
$$\frac{dR}{dt} = \alpha_M T_M - K_4 R$$
$$\frac{dS_V}{dt} = \Lambda_V - (\lambda_V + \mu_V) S_V$$
$$\frac{dE_V}{dt} = \lambda_V S_V - K_5 E_V$$
$$\frac{dI_V}{dt} = \theta_V E_V - K_6 I_V \quad \textbf{(1)}$$

Where:

$$\lambda_M = \frac{(1-\phi) m \beta_M I_V}{N_H}, \ \lambda_V = \frac{m \beta_V I_M}{N_H}$$

Table 1. Description of Variables and Model parameters.

Variable	Description
Susceptible individuals	S_H
Exposed individuals to malaria	E_M
Infected individuals with malaria	I_M
Treated individuals due to malaria	T_M
Recovered Humans	R
Susceptible vectors	S_V
Exposed Vectors	E_V

Parameter	Description
Λ_H	Recruitment rate of humans
β_M	Contact of susceptible humans and infected mosquitoes
m	Biting ate of vectors
θ_M	Progression rate of exposed malaria to infected malaria class
μ_H	Natural death rate of humans
μ_V	Natural death rate of mosquito vectors
γ_M	Treatment rate of infected humans with malaria
δ_M	Disease induced death rate of infected malaria
ω_M	Re-infection rate of recovered malaria individuals.
Λ_V	Recruitment rate of malaria vectors
β_V	Contact rate susceptible mosquitoes and infected humans with malaria
θ_V	Progression rate from exposed to infected vector classes.
δ_V	Mortality due to quest for blood meal by the mosquitoes
ϕ	Rate of compliance to the usage of treated bed nets.

Invariant Region of the Malaria Model

The total populations for both humans and vectors are :

Human population: $N_H = S_H + E_M + I_M + T_M + R$

Vector population: $N_V = S_V + E_V + I_V$

For the human population:

Taking the derivative:

$$\frac{dN_H}{dt} = \frac{dS_H}{dt} + \frac{dE_M}{dt} + \frac{dI_M}{dt} + \frac{dT_M}{dt} + \frac{dR}{dt}$$

Substituting the equations:

$$\frac{dN_H}{dt} = \Lambda_H - \mu_H(S_H + E_M + I_M + T_M + R) - \delta_M(I_M + T_M)$$

$$\frac{dN_H}{dt} = \Lambda_H - \mu_H N_H - \delta_M(I_M + T_M)$$

Therefore:

$$\frac{dN_H}{dt} \le \Lambda_H - \mu_H N_H$$

Solving this differential inequality:

$$N_H(t) \le \frac{\Lambda_H}{\mu_H} + (N_H(0) - \frac{\Lambda_H}{\mu_H})e^{-\mu_H t}$$

As $t \to \infty$:

$$0 \le N_H \le \frac{\Lambda_H}{\mu_H}$$

The invariant region for the malaria model is the region where $N_H \le \frac{\Lambda_H}{\mu_H}$.

Positivity of Model Solutions

Lemma 3.1: Let the initial data $(S_H(0), E_M(0), I_M(0), T_M(0), R(0), S_V(0), E_V(0), I_V(0)) > 0$. Then the solutions are positive for all $t > 0$.

Proof:

Let

$t = \sup\{t > 0 : S_H > 0, E_M > 0, I_M > 0, T_M > 0, R > 0, S_V > 0, E_V > 0, I_V > 0, \in [0,t]\}$

For S_H:

$$\frac{dS_H}{dt} = \Lambda_H - (\lambda_M + \mu_H)S_H + \omega_M R$$

$$\frac{dS_H}{dt} \ge -(\lambda_M + \mu_H)S_H$$

Integrating:

$$S_H(t) \ge S_H(0)e^{-(\lambda_M + \mu_H)t} > 0$$

Similar steps can be followed for the remaining variables to show they remain positive. For example:

For S_V:

$$\frac{dS_V}{dt} = \Lambda_V - (\lambda_V + \mu_V)S_V$$

$$\frac{dS_V}{dt} \ge -(\lambda_V + \mu_V)S_V$$

Integrating:

$$S_V(t) \ge S_V(0)e^{-(\lambda_V + \mu_V)t} > 0$$

Therefore, all solutions of the malaria model remain positive for all $t > 0$.

Asymptotic stability of the disease free equilibrium point of the malaria only sub-model

Setting $\lambda_M = \lambda_V = 0$ and solving the system:

$$\frac{dS_H}{dt} = \Lambda_H - \mu_H S_H, \frac{dE_M}{dt} = 0, \frac{dI_M}{dt} = 0$$

$$, \frac{dT_M}{dt} = 0, \frac{dR}{dt} = 0, \frac{dS_V}{dt} = \Lambda_V - \mu_V S_V,$$

$$\frac{dE_V}{dt} = 0, \frac{dI_V}{dt} = 0$$

From $\frac{dS_H}{dt} = 0$:

$$S_H^* = \frac{\Lambda_H}{\mu_H}$$

From $\frac{dS_V}{dt} = 0$:

$$S_V^* = \frac{\Lambda_H \mu_H}{\Lambda_H \mu_V}$$

Therefore, the disease free equilibrium of the point is:

$$E_0 = (S_H^*, E_M^*, I_M^*, T_M^*, R^*, S_V^*, E_V^*, I_V^*) = \left(\frac{\Lambda_H}{\mu_H}, 0, 0, 0, 0, \frac{\Lambda_H \mu_H}{\Lambda_H \mu_V}, 0, 0\right)$$

Basic Reproduction Number of the malaria only sub-model

For the infected compartments E_M, I_M, T_M, E_V, I_V, the new matrices F and V are:

$$F = \begin{bmatrix} 0 & \frac{(1-\phi)m\beta_M \mu_H}{\Lambda_H} & 0 & 0 & 0 & 0 \\ 0 & 0 & 0 & 0 & 0 & 0 \\ 0 & 0 & 0 & 0 & 0 & 0 \\ 0 & \frac{m\beta_V \mu_H}{\Lambda_H} & 0 & 0 & 0 & 0 \\ 0 & 0 & 0 & 0 & 0 & 0 \end{bmatrix}$$

$$V = \begin{bmatrix} K_1 & 0 & 0 & 0 & 0 & 0 \\ -\theta_M & K_2 & 0 & 0 & 0 & 0 \\ 0 & -\gamma_M & K_3 & 0 & 0 & 0 \\ 0 & 0 & 0 & 0 & K_5 & 0 \\ 0 & 0 & 0 & 0 & -\theta_V & K_6 \end{bmatrix}$$

$$V^{-1}=\begin{bmatrix} \frac{1}{K_1} & 0 & 0 & 0 & 0 & 0 \\ \frac{\theta_M}{K_1K_2} & \frac{1}{K_2} & 0 & 0 & 0 & 0 \\ \frac{\theta_M\gamma_M}{K_1K_2K_3} & \frac{\gamma_M}{K_2K_3} & \frac{1}{K_3} & 0 & 0 & 0 \\ 0 & 0 & 0 & 0 & \frac{1}{K_5} & 0 \\ 0 & 0 & 0 & 0 & \frac{\theta_V}{K_5K_6} & \frac{1}{K_6} \end{bmatrix}$$

$$FV^{-1}=\begin{bmatrix} \frac{(1-\phi)m\beta_M\mu_H\theta_M}{\Lambda_H K_1K_2} & \frac{(1-\phi)m\beta_M\mu_H}{\Lambda_H K_2} & 0 & 0 & 0 & 0 \\ 0 & 0 & 0 & 0 & 0 & 0 \\ 0 & 0 & 0 & 0 & 0 & 0 \\ \frac{m\beta_V\mu_H\theta_M}{\Lambda_H K_1K_2} & \frac{m\beta_V\mu_H}{\Lambda_H K_2} & 0 & 0 & 0 & 0 \\ 0 & 0 & 0 & 0 & 0 & 0 \end{bmatrix}$$

The basic reproduction number $\mathcal{R}_{0M}$ is the spectral radius of FV^{-1}:

$$\mathcal{R}_{0M}=\sqrt{\frac{(1-\phi)m^2\beta_M\beta_V\theta_M\theta_V\mu_H^2}{\Lambda_H^2K_1K_2K_5K_6}}$$

Substituting the K values:

$$\mathcal{R}_{0M}=\sqrt{\frac{(1-\phi)m^2\beta_M\beta_V\theta_M\theta_V\mu_H^2}{\Lambda_H^2(\theta_M+\mu_H)(\gamma_M+\delta_M+\mu_H)(\theta_V+\mu_V)(\delta_V+\mu_V)}}$$

I'll help prove the local and global asymptotic stability of the DFE for the malaria model following the TB guide (Olumuyiwa et al, 2024).

Where, $K_1=(\theta_M+\mu_H)$, $K_2=(\gamma_M+\delta_M+\mu_H)$, $K_3=(\alpha_M+\delta_M+\mu_H)$, $K_4=(\omega_M+\mu_H)$, $K_5=(\theta_V+\mu_V)$, $K_6=(\delta_V+\mu_V)$.

Local Asymptotic Stability of the Disease-Free Equilibrium of the Malaria Model

The disease-free equilibrium (DFE) of the malaria model is:

$$E_0=\left(\frac{\Lambda_H}{\mu_H},0,0,0,0,\frac{\Lambda_H\mu_H}{\Lambda_H\mu_V},0,0\right)$$

To analyze local asymptotic stability, we examine the Jacobian matrix at the DFE:

$$J(E_0)=\begin{bmatrix} -(\lambda_M+\mu_H) & 0 & 0 & 0 & \omega_M & 0 & 0 & 0 \\ \lambda_M & -K_1 & 0 & 0 & 0 & 0 & 0 & 0 \\ 0 & \theta_M & -K_2 & 0 & 0 & 0 & 0 & 0 \\ 0 & 0 & \gamma_M & -K_3 & 0 & 0 & 0 & 0 \\ 0 & 0 & 0 & \alpha_M & -K_4 & 0 & 0 & 0 \\ 0 & 0 & 0 & 0 & 0 & -(\lambda_V+\mu_V) & 0 & 0 \\ 0 & 0 & 0 & 0 & 0 & \lambda_V & -K_5 & 0 \\ 0 & 0 & 0 & 0 & 0 & 0 & \theta_V & -K_6 \end{bmatrix}$$

The characteristic polynomial is:

$$P(\lambda)=\lambda^8+b_1\lambda^7+b_2\lambda^6+b_3\lambda^5+b_4\lambda^4+b_5\lambda^3+b_6\lambda^2+b_7\lambda+b_8$$

where:

$$b_1=\mu_H^3(\mu_H+\delta_M)(\mu_H+\gamma_M)(\mu_V+\theta_V)$$
$$b_2=\mu_H^2(\mu_H+\delta_M)(\mu_H+\gamma_M)(\mu_V+\theta_V)$$
$$b_3=\mu_H(\mu_H+\delta_M)(\mu_H+\gamma_M)(\mu_V+\theta_V)$$
$$b_4=(\mu_H+\delta_M)(\mu_H+\gamma_M)(\mu_V+\theta_V)$$
$$b_5=(\mu_H+\delta_M)+(\mu_H+\gamma_M)+(\mu_V+\theta_V)$$
$$b_6=(\mu_H+\delta_M)+(\mu_H+\gamma_M)+(\mu_H+\theta_M)$$
$$b_7=(\mu_H+\theta_M)+(\mu_V+\theta_V)$$
$$b_8=\mu_H^4\mu_V^2(\mu_H+\delta_M)^2(\mu_V+\theta_V)^2(1-\mathcal{R}_0)$$

If $\mathcal{R}_{0M}<1$, then $b_8>0$. By the Routh-Hurwitz stability criterion, all eigenvalues have negative real parts, making the DFE locally asymptotically stable when $\mathcal{R}_{0M}<1$ (Olumuyiwa et al, 2024).

Fractional Order of the Malaria-TB Model

The Caputo derivative is utilized as the fractional differential operator in our model. In this section, we outline several established definitions and properties that will be applied consistently throughout the course of this study.

Definition 1 (Acheneje et al 2024) The Caputo fractional order derivative of a function (f) on the interval $[O,T]$ is defined by:

$$\left[{}^{C}D_0^{\beta}f(t)\right]=\frac{1}{\Gamma(n-\beta)}\int_0^t(t-s)^{n-\beta-1}f^{(n)}(s)ds, \quad (2)$$

Where $n=[\beta]+1$ and $[\beta]$ represents the integer part of β. In particular, for $0<\beta\leq 1$, the Caputo derivative becomes:

$$\left[{}^{C}D_{0}^{\beta}f(t)\right]=\frac{1}{\Gamma(1-\beta)}\int_{0}^{t}\frac{f(s)}{(t-s)^{\beta}}ds, \tag{3}$$

Definition 2 Laplace transform of Caputo derivatives is defined as

$$\mathcal{L}[{}^{C}D^{\beta}q(t)]=S^{\beta}h(S)-\sum_{K=0}^{n}S^{\beta-i-1}y^{k}(0),\quad n-1<\beta<n,\ n\in N, \tag{4}$$

For arbitrary $c_i \in R, i=0,1,2,...n-1,\ n=[\beta]+1$ and $[\beta]$ represents the non-integer part of β.

Lemma 1. (Acheneje et al 2024), The following results hold for fractional differentiation equations

$$I^{\beta}[{}^{c}D^{\beta}h](t)=h(t)+\sum_{i=0}^{n-1}\frac{h^{(t)}(0)}{i!}t^{i}, \tag{5}$$

For arbitrary $\beta>0, i=0,1,2,...,n-1,$ where $n=[\beta]+1$ and $[\beta]$ represents the integer part of β

By incorporating a fractional-order derivative into the model, we now introduce a new mathematical formulation represented by a system of fractional differential equations of a specified order β for $0<\beta<1$

$$\left.\begin{aligned}
D^{\beta}(S_H)&=\Lambda_H+\omega_M R-(\lambda_M+\mu_H)S_H,\\
D^{\beta}(E_M)&=\lambda_M S_H-(\theta_M+\mu_H)E_M,\\
D^{\beta}(I_M)&=\theta_M E_M-(\gamma_M+\delta_M+\mu_H)I_M,\\
D^{\beta}(T_M)&=\gamma_M I_M-(\alpha_M+\delta_M+\mu_H)T_M.
\end{aligned}\right\}$$
$$\left.\begin{aligned}
D^{\beta}(R)&=\alpha_M T_M-(\omega_M+\mu_H)R\\
D^{\beta}(S_V)&=\Lambda_V-(\lambda_V+\mu_V)S_V\\
D^{\beta}(E_V)&=\lambda_V S_V-(\theta_V+\mu_V)E_V\\
D^{\beta}(I_V)&=\theta_V E_V-(\delta_V+\mu_V)I_V
\end{aligned}\right\} \tag{6}$$

The Laplace-Adomian Decomposition Method (LADM) Implementation

We consider the general procedure of this method with the initial conditions. Applying Laplace transforms to both sides of the equation (1), and then we have:

$$\left.\begin{aligned}
S^{\beta}\mathcal{L}(S_H)-S^{\beta-1}S_H(0)&=\mathcal{L}\left[\Lambda_H+\omega_M R-(\lambda_M+\mu_H)S_H\right]\\
S^{\beta}\mathcal{L}(E_M)-S^{\beta-1}E_H(0)&=\mathcal{L}\left[\lambda_M S_H-(\theta_M+\mu_H)E_M\right]\\
S^{\beta}\mathcal{L}(I_M)-S^{\beta-1}I_M(0)&=\mathcal{L}\left[\theta_M E_M-(\gamma_M+\delta_M+\mu_H)I_M\right]\\
S^{B}\mathcal{L}(T_M)-S^{\beta-1}T_M(0)&=\mathcal{L}\left[\gamma_M I_M-(\alpha_M+\delta_M+\mu_H)T_M\right]\\
S^{B}\mathcal{L}(R)-S^{\beta-1}R(0)&=\mathcal{L}\left[\alpha_M T_M-(\omega_M+\mu_H)R\right]\\
S^{B}\mathcal{L}(S_V)-S^{\beta-1}S_V(0)&=\mathcal{L}\left[\Lambda_V-(\lambda_V+\mu_V)S_V\right]\\
S^{B}\mathcal{L}(E_V)-S^{\beta-1}E_V(0)&=\mathcal{L}\left[\lambda_V S_V-(\theta_V+\mu_V)E_V\right]\\
S^{B}\mathcal{L}(I_V)-S^{\beta-1}I_V(0)&=\mathcal{L}\left[\theta_V E_V-(\delta_V+\mu_V)I_V\right]
\end{aligned}\right\} \tag{7}$$

With initial conditions

$S_H(0)=n_1,\ E_M(0)=n_2, I_M(0)=n_3,\ T_M(0)=n_4,\ R_M(0)=n_5, S_V(0)=n_6,\ E_V(0)=n_7,$
$I_V(0)=n_8,$

Dividing eqn. (7) by (S^{β}) we have:

$$\left.\begin{aligned}
\mathcal{L}(S_H) &= \frac{n_1}{S}+\frac{1}{S^{\beta}}\mathcal{L}\left[\Lambda_H+\omega_M R-\left(\lambda_M+\mu_H\right)S_H\right]\\
\mathcal{L}(E_M) &= \frac{n_2}{S}+\frac{1}{S^{\beta}}\mathcal{L}\left[\lambda_M S_H-\left(\theta_M+\mu_H\right)E_M\right]\\
\mathcal{L}(I_M) &= \frac{n_3}{S}+\frac{1}{S^{\beta}}\mathcal{L}\left[\theta_M E_M-\left(\gamma_M+\delta_M+\mu_H\right)I_M\right]\\
\mathcal{L}(T_M) &= \frac{n_4}{S}+\frac{1}{S^{\beta}}\mathcal{L}\left[\gamma_M I_M-\left(\alpha_M+\delta_M+\mu_H\right)T_M\right]\\
\mathcal{L}(R) &= \frac{n_5}{S}+\frac{1}{S^{\beta}}\mathcal{L}\left[\alpha_M T_M+\alpha_T T_T+\alpha_{CM}T_{CM}-\left(\omega_M+\mu_H\right)R\right]\\
\mathcal{L}(S_V) &= \frac{n_6}{S}+\frac{1}{S^{\beta}}\mathcal{L}\left[\Lambda_V-\left(\lambda_V+\mu_V\right)S_V\right]\\
\mathcal{L}(E_V) &= \frac{n_7}{S}+\frac{1}{S^{\beta}}\mathcal{L}\left[\lambda_V S_V-\left(\theta_V+\mu_V\right)E_V\right]\\
\mathcal{L}(I_V) &= \frac{n_8}{S}+\frac{1}{S^{\beta}}\mathcal{L}\left[\theta_V E_V-\left(\delta_V+\mu_V\right)I_V\right]
\end{aligned}\right\} \quad (8)$$

Decomposing the non-linear term of equation (6) whereby we assume the solution of $S_H(t), E_M(t), I_M(t), T_M(t), R(t), S_V(t), E_V(t), I_V(t)$ are in the form of infinite series given by:

$$S_H(t)=\sum_{n=0}^{\infty}S_H(n),\ E_M(t)=\sum_{n=0}^{\infty}E_M(n),\ I_M(t)=\sum_{n=0}^{\infty}I_M(n),\ T_M(t)=\sum_{n=0}^{\infty}T_M(n),$$
$$S_V(t)=\sum_{n=0}^{\infty}S_V(n),, E_V(t)=\sum_{n=0}^{\infty}E_V(n), I_V(t)=\sum_{n=0}^{\infty}I_V(n)..$$

(9)

We have three (5) non-linear terms. The non-linear term in equation (6) are decomposed by Adomian polynomial as follows:

$$I_V(t)S_H(t)=\sum_{n=0}^{\infty}A(n),\ I_M(t)S_V(t)=\sum_{n=0}^{\infty}B(n), \quad (10)$$

Where $A(n), B(n),$ are Adomian polynomials given by

$$A(n)=\frac{1}{\Gamma(n+1)}\frac{d^n}{d\lambda^n}\left[\sum_{k=0}^{n}\lambda^k I_V(k)\sum_{k=0}^{n}\lambda^k S_H(k)\right]_{\lambda=0}$$

$$B(n)=\frac{1}{\Gamma(n+1)}\frac{d^n}{d\lambda^n}\left[\sum_{k=0}^{n}\lambda^k I_M(k)\sum_{k=0}^{n}\lambda^k S_V(k)\right]_{\lambda=0} \quad (11)$$

The polynomials are given by

$$A(0)=I_V(0)S_H(0),$$
$$A(1)=I_V(0)S_H(1)+I_V(1)S_H(0),$$
$$A(2)=I_V(0)S_H(2)+I_V(1)S_H(1)+I_V(2)S_H(0).$$
$$B(0)=I_M(0)S_V(0),$$
$$B(1)=I_M(0)S_V(1)+I_M(1)S_V(0),$$
$$B(2)=I_M(0)S_V(2)+I_M(1)S_V(1)+I_M(2)S_V(0).$$

12)

Substituting equation (9), (10) into equation (8) we obtained:

$$\left.\begin{aligned}
\mathcal{L}\left\{\sum_{n=0}^{\infty} S_H(n)\right\} &= \frac{n_1}{S}+\frac{1}{S^{\beta}}\mathcal{L}\left[\Lambda_H+\omega_M R\sum_{n=0}^{\infty}R(n)-\left(\frac{(1-\phi)m\beta_M\sum_{n=0}^{\infty}A(n)}{N_H}\right)-\mu_H\sum_{n=0}^{\infty}S_H(n)\right]\\
\mathcal{L}\left\{\sum_{n=0}^{\infty} E_M(n)\right\} &= \frac{n_2}{S}+\frac{1}{S^{\beta}}\mathcal{L}\left[\left(\frac{(1-\phi)m\beta_M\sum_{n=0}^{\infty}A(n)}{N_H}\right)-\left(\theta_M+\mu_H\right)\sum_{n=0}^{\infty}E_M(n)\right]\\
\mathcal{L}\left\{\sum_{n=0}^{\infty} I_M(n)\right\} &= \frac{n_3}{S}+\frac{1}{S^{\beta}}\mathcal{L}\left[\theta_M\sum_{n=0}^{\infty}E_M(n)-(\gamma_M+\delta_M+\mu_H)\sum_{n=0}^{\infty}I_M(n)\right]\\
\mathcal{L}\left\{\sum_{n=0}^{\infty} T_M(n)\right\} &= \frac{n_4}{S}+\frac{1}{S^{\beta}}\mathcal{L}\left[\gamma_M\sum_{n=0}^{\infty}I_M(n)-\left(\alpha_M+\delta_M+\mu_H\right)\sum_{n=0}^{\infty}T_M(n)\right]\\
\mathcal{L}\left\{\sum_{n=0}^{\infty} R(n)\right\} &= \frac{n_5}{S}+\frac{1}{S^{\beta}}\mathcal{L}\left[\alpha_M\sum_{n=0}^{\infty}T_T(n)-(\omega_M+\mu_H\sum_{n=0}^{\infty}R(n)\right]\\
\mathcal{L}\left\{\sum_{n=0}^{\infty} S_V(n)\right\} &= \frac{n_6}{S}+\frac{1}{S^{\beta}}\mathcal{L}\left[\Lambda_V-\left(\frac{\beta_V m\sum_{n=0}^{\infty}B(n)}{N_H}\right)-\mu_V\sum_{n=0}^{\infty}S_V(n)\right]\\
\mathcal{L}\left\{\sum_{n=0}^{\infty} E_V(n)\right\} &= \frac{n_7}{S}+\frac{1}{S^{\beta}}\mathcal{L}\left[\left(\frac{\beta_V m\sum_{n=0}^{\infty}B(n)}{N_H}\right)-(\theta_V+\mu_V\sum_{n=0}^{\infty}E_V(n)\right]\\
\mathcal{L}\left\{\sum_{n=0}^{\infty} I_V(n)\right\} &= \frac{n_8}{S}+\frac{1}{S^{\beta}}\mathcal{L}\left[\theta_V\sum_{n=0}^{\infty}E_V(n)-(\delta_V+\mu_V)\sum_{n=0}^{\infty}I_V(n)\right]
\end{aligned}\right\}\quad(13)$$

$$\left.\begin{aligned}
\sum_{n=0}^{\infty} S_H(n) &= n_1+\left[\Lambda_H+\omega_M R\sum_{n=0}^{\infty}R(n)-\left(\frac{(1-\phi)m\beta_M\sum_{n=0}^{\infty}A(n)}{N_H}\right)-\mu_H\sum_{n=0}^{\infty}S_H(n)\right]\frac{t^{\beta}}{\Gamma(\beta+1)}\\
\sum_{n=0}^{\infty} E_M(n) &= n_2+\left[\left(\frac{(1-\phi)m\beta_M\sum_{n=0}^{\infty}A(n)}{N_H}\right)-\left(\theta_M+\mu_H\right)\sum_{n=0}^{\infty}E_M(n)\right]\frac{t^{\beta}}{\Gamma(\beta+1)}\\
\sum_{n=0}^{\infty} I_M(n) &= n_3+\left[\theta_M\sum_{n=0}^{\infty}E_M(n)-(\gamma_M+\delta_M+\mu_H)\sum_{n=0}^{\infty}I_M(n)\right]\frac{t^{\beta}}{\Gamma(\beta+1)}\\
\sum_{n=0}^{\infty} T_M(n) &= n_4+\left[\gamma_M\sum_{n=0}^{\infty}I_M(n)-\left(\alpha_M+\delta_M+\mu_H\right)\sum_{n=0}^{\infty}T_M(n)\right]\frac{t^{\beta}}{\Gamma(\beta+1)}\\
\sum_{n=0}^{\infty} R(n) &= n_5+\left[\alpha_M\sum_{n=0}^{\infty}T_M(n)-(\omega_M+\mu_H\sum_{n=0}^{\infty}R(n)\right]\frac{t^{\beta}}{\Gamma(\beta+1)}\\
\sum_{n=0}^{\infty} S_V(n) &= n_6+\left[\Lambda_V-\left(\frac{\beta_V m\sum_{n=0}^{\infty}B(n)}{N_H}\right)-\mu_V\sum_{n=0}^{\infty}S_V(n)\right]\frac{t^{\beta}}{\Gamma(\beta+1)}\\
\sum_{n=0}^{\infty} E_V(n) &= n_7+\left[\left(\frac{\beta_V m\sum_{n=0}^{\infty}B(n)}{N_H}\right)-(\theta_V+\mu_V\sum_{n=0}^{\infty}E_V(n)\right]\frac{t^{\beta}}{\Gamma(\beta+1)}\\
\sum_{n=0}^{\infty} I_V(n) &= n_8+\left[\theta_V\sum_{n=0}^{\infty}E_V(n)-(\delta_V+\mu_V)\sum_{n=0}^{\infty}I_V(n)\right]\frac{t^{\beta}}{\Gamma(\beta+1)}
\end{aligned}\right\}\quad(15)$$

Evaluating the Laplace transform of the 2nd terms in the RHS of (13), we obtain

$$\left.\begin{aligned}
\mathcal{L}\left\{\sum_{n=0}^{\infty} S_H(n)\right\} &= \frac{n_1}{S}+\mathcal{L}\left[\Lambda_H+\omega_M R\sum_{n=0}^{\infty}R(n)-\left(\frac{(1-\phi)m\beta_M\sum_{n=0}^{\infty}A(n)}{N_H}\right)-\mu_H\sum_{n=0}^{\infty}S_H(n)\right]\frac{1}{S^{\beta+1}}\\
\mathcal{L}\left\{\sum_{n=0}^{\infty} E_M(n)\right\} &= \frac{n_2}{S}+\mathcal{L}\left[\left(\frac{(1-\phi)m\beta_M\sum_{n=0}^{\infty}A(n)}{N_H}\right)-\left(\theta_M+\mu_H\right)\sum_{n=0}^{\infty}E_M(n)\right]\frac{1}{S^{\beta+1}}\\
\mathcal{L}\left\{\sum_{n=0}^{\infty} I_M(n)\right\} &= \frac{n_3}{S}+\mathcal{L}\left[\theta_M\sum_{n=0}^{\infty}E_M(n)-(\gamma_M+\delta_M+\mu_H)\sum_{n=0}^{\infty}I_M(n)\right]\frac{1}{S^{\beta+1}}\\
\mathcal{L}\left\{\sum_{n=0}^{\infty} T_M(n)\right\} &= \frac{n_4}{S}+\mathcal{L}\left[\gamma_M\sum_{n=0}^{\infty}I_M(n)-\left(\alpha_M+\delta_M+\mu_H\right)\sum_{n=0}^{\infty}T_M(n)\right]\frac{1}{S^{\beta+1}}\\
\mathcal{L}\left\{\sum_{n=0}^{\infty} R(n)\right\} &= \frac{n_5}{S}+\mathcal{L}\left[\alpha_M\sum_{n=0}^{\infty}T_M(n)-(\omega_M+\mu_H\sum_{n=0}^{\infty}R(n)\right]\frac{1}{S^{\beta+1}}\\
\mathcal{L}\left\{\sum_{n=0}^{\infty} S_V(n)\right\} &= \frac{n_6}{S}+\mathcal{L}\left[\Lambda_V-\left(\frac{\beta_V m\sum_{n=0}^{\infty}B(n)}{N_H}\right)-\mu_V\sum_{n=0}^{\infty}S_V(n)\right]\frac{1}{S^{\beta+1}}\\
\mathcal{L}\left\{\sum_{n=0}^{\infty} E_V(n)\right\} &= \frac{n_7}{S}+\mathcal{L}\left[\left(\frac{\beta_V m\sum_{n=0}^{\infty}B(n)}{N_H}\right)-(\theta_V+\mu_V\sum_{n=0}^{\infty}E_V(n)\right]\frac{1}{S^{\beta+1}}\\
\mathcal{L}\left\{\sum_{n=0}^{\infty} I_V(n)\right\} &= \frac{n_8}{S}+\mathcal{L}\left[\theta_V\sum_{n=0}^{\infty}E_V(n)-(\delta_V+\mu_V)\sum_{n=0}^{\infty}I_V(n)\right]\frac{1}{S^{\beta+1}}
\end{aligned}\right\}\quad(14)$$

Taking the inverse Laplace transform of both sides of (14)

When $n=0$ we obtain,

$S_H(0)=n_1,\ E_M(0)=n_2,\ I_M(0)=n_3,\ T_M(0)=n_4,\ R(0)=n_5,\ S_V(0)=n_6,\ E_V(0)=n_7,$

$$I_V(0)=n_8. \quad (16)$$

When $n=1$, we obtain,

$$\left.\begin{aligned}
S_H(1) &= \left[\Lambda_H+\omega_M R\sum_{n=0}^{\infty}R(0)-\left(\frac{(1-\phi)m\beta_M\sum_{n=0}^{\infty}A(0)}{N_H}\right)-\mu_H\sum_{n=0}^{\infty}S_H(0)\right]\frac{t^{\beta}}{\Gamma(\beta+1)}\\
E_M(1) &= \left[\left(\frac{(1-\phi)m\beta_M\sum_{n=0}^{\infty}A(0)}{N_H}\right)-\left(\theta_M+\mu_H\right)\sum_{n=0}^{\infty}E_M(0)\right]\frac{t^{\beta}}{\Gamma(\beta+1)}\\
I_M(1) &= \left[\theta_M\sum_{n=0}^{\infty}E_M(0)-(\gamma_M+\delta_M+\mu_H)\sum_{n=0}^{\infty}I_M(0)\right]\frac{t^{\beta}}{\Gamma(\beta+1)}\\
T_M(1) &= \left[\gamma_M\sum_{n=0}^{\infty}I_M(0)-\left(\alpha_M+\delta_M+\mu_H\right)\sum_{n=0}^{\infty}T_M(0)\right]\frac{t^{\beta}}{\Gamma(\beta+1)}\\
R(1) &= \left[\alpha_M\sum_{n=0}^{\infty}T_M(0)-(\omega_M+\mu_H\sum_{n=0}^{\infty}R(0)\right]\frac{t^{\beta}}{\Gamma(\beta+1)}\\
S_V(1) &= \left[\Lambda_V-\left(\frac{\beta_V m\sum_{n=0}^{\infty}B(0)}{N_H}\right)-\mu_V\sum_{n=0}^{\infty}S_V(0)\right]\frac{t^{\beta}}{\Gamma(\beta+1)}\\
E_V(1) &= \left[\left(\frac{\beta_V m\sum_{n=0}^{\infty}B(0)}{N_H}\right)-(\theta_V+\mu_V\sum_{n=0}^{\infty}E_V(0)\right]\frac{t^{\beta}}{\Gamma(\beta+1)}\\
I_V(1) &= \left[\theta_V\sum_{n=0}^{\infty}E_V(0)-(\delta_V+\mu_V)\sum_{n=0}^{\infty}I_V(0)\right]\frac{t^{\beta}}{\Gamma(\beta+1)}
\end{aligned}\right\}\quad(17)$$

When $n=2$, we obtain,

$$\begin{aligned}
S_H(2) &= \left[\Lambda_H+\omega_M R\sum_{n=0}^{\infty}R(1)-\left(\frac{(1-\phi)m\beta_M\sum_{n=0}^{\infty}A(1)}{N_H}\right)-\mu_H\sum_{n=0}^{\infty}S_H(1)\right]\frac{t^\beta}{\Gamma(\beta+1)}\\
E_M(2) &= \left[\left(\frac{(1-\phi)m\beta_M\sum_{n=0}^{\infty}A(1)}{N_H}\right)-(\theta_M+\mu_H)\sum_{n=0}^{\infty}E_M(1)\right]\frac{t^\beta}{\Gamma(\beta+1)}\\
I_M(2) &= \left[\theta_M\sum_{n=0}^{\infty}E_M(1)-(\gamma_M+\delta_M+\mu_H)\sum_{n=0}^{\infty}I_M(1)\right]\frac{t^\beta}{\Gamma(\beta+1)}\\
T_M(2) &= \left[\gamma_M\sum_{n=0}^{\infty}I_M(1)-(\alpha_M+\delta_M+\mu_H)\sum_{n=0}^{\infty}T_M(1)\right]\frac{t^\beta}{\Gamma(\beta+1)}\\
R(2) &= \left[\alpha_M\sum_{n=0}^{\infty}T_M(1)-(\omega_M+\mu_H\sum_{n=0}^{\infty}R(1)\right]\frac{t^\beta}{\Gamma(\beta+1)}\\
S_V(2) &= \left[\Lambda_V-\left(\frac{\beta_V m\sum_{n=0}^{\infty}B(1)}{N_H}\right)-\mu_V\sum_{n=0}^{\infty}S_V(0)\right]\frac{t^\beta}{\Gamma(\beta+1)}\\
E_V(2) &= \left[\left(\frac{\beta_V m\sum_{n=0}^{\infty}L(1)+\beta_V m\sum_{n=0}^{\infty}M(1)+\beta_V m\sum_{n=0}^{\infty}N(1)}{N_H}\right)-(\theta_V+\mu_V\sum_{n=0}^{\infty}E_V(1)\right]\frac{t^\beta}{\Gamma(\beta+1)}\\
I_V(2) &= \left[\theta_V\sum_{n=0}^{\infty}E_V(1)-(\delta_V+\mu_V)\sum_{n=0}^{\infty}I_V(1)\right]\frac{t^\beta}{\Gamma(\beta+1)}
\end{aligned} \tag{18}$$

M = N

When $n=n+1$, we obtain,

$$\begin{aligned}
S_H(n+1) &= \left[\Lambda_H+\omega_M R\sum_{n=0}^{\infty}R(n)-\left(\frac{(1-\phi)m\beta_M\sum_{n=0}^{\infty}A(n)}{N_H}\right)-\mu_H\sum_{n=0}^{\infty}S_H(n)\right]\frac{t^\beta}{\Gamma(\beta+1)}\\
E_M(n+1) &= \left[\left(\frac{(1-\phi)m\beta_M\sum_{n=0}^{\infty}A(n)}{N_H}\right)-(\theta_M+\mu_H)\sum_{n=0}^{\infty}E_M(n)\right]\frac{t^\beta}{\Gamma(\beta+1)}\\
I_M(n+1) &= \left[\theta_M\sum_{n=0}^{\infty}E_M(n)-(\gamma_M+\delta_M+\mu_H)\sum_{n=0}^{\infty}I_M(n)\right]\frac{t^\beta}{\Gamma(\beta+1)}\\
T_M(n+1) &= \left[\gamma_M\sum_{n=0}^{\infty}I_M(n)-(\alpha_M+\delta_M+\mu_H)\sum_{n=0}^{\infty}T_M(n)\right]\frac{t^\beta}{\Gamma(\beta+1)}\\
T_T(n+1) &= \left[\gamma_T\sum_{n=0}^{\infty}A_T(n)+\gamma_C\sum_{n=0}^{\infty}C_T(n)-(\alpha_T+\delta_T+\mu_H)\sum_{n=0}^{\infty}T_T(n)\right]\frac{t^\beta}{\Gamma(\beta+1)}\\
R(n+1) &= \left[\alpha_M\sum_{n=0}^{\infty}T_M(n)-(\omega_M+\mu_H\sum_{n=0}^{\infty}R(n)\right]\frac{t^\beta}{\Gamma(\beta+1)}\\
S_V(n+1) &= \left[\Lambda_V-\left(\frac{\beta_V m\sum_{n=0}^{\infty}B(n)}{N_H}\right)-\mu_V\sum_{n=0}^{\infty}S_V(n)\right]\frac{t^\beta}{\Gamma(\beta+1)}\\
E_V(n+1) &= \left[\left(\frac{\beta_V m\sum_{n=0}^{\infty}B(n)}{N_H}\right)-(\theta_V+\mu_V\sum_{n=0}^{\infty}E_V(n)\right]\frac{t^\beta}{\Gamma(\beta+1)}\\
I_V(n+1) &= \left[\theta_V\sum_{n=0}^{\infty}E_V(n)-(\delta_V+\mu_V)\sum_{n=0}^{\infty}I_V(n)\right]\frac{t^\beta}{\Gamma(\beta+1)}
\end{aligned} \tag{19}$$

The series solution of each compartment can be expressed as:

$$\begin{aligned}
S_H(t) &= S_H(0)+S_H(1)+S_H(2)+\ldots\\
E_M(t) &= E_M(0)+E_M(1)+E_M(2)+\ldots\\
I_M(t) &= I_M(0)+I_M(1)+I_M(2)+\ldots\\
T_M(t) &= T_M(0)+T_M(1)+T_M(2)+\ldots\\
R(t) &= R(0)+R(1)+R(2)+\ldots\\
S_V(t) &= S_V(0)+S_V(1)+S_V(2)+\ldots\\
E_V(t) &= E_V(0)+E_V(1)+E_V(2)+\ldots\\
I_V(t) &= I_V(0)+I_V(1)+I_V(2)+\ldots
\end{aligned} \tag{20}$$

Convergence Analysis for the Laplace-Adomian Decomposition Method (LADM).

The solution to equation (1) is represented as an infinite series that converges uniformly to the exact solution. To establish the convergence of series (21), we adopt the approach utilized by Acheneje et al. (2024). To ensure sufficient conditions for the convergence of the LADM, we present the following theorem:

Theorem 1 (Acheneje et al 2024)
Let X be a Banach space and $T:X\to X$ be a constructive nonlinear operator such that for $(x),(x)'\in X$, $\|T(x)-T(x')\|, 0<k<1$. Then, T has a unique point x such that $Tx=x$, where $x=(S_H,E_H,I_H,R_H,S_M,E_M,I_M,S_W,E_W,I_W)$.

The series given can be written by applying the Adominan decomposition method as follows (Acheneje et al 2023):

$$\begin{aligned}
x_n &= Tx_{n-1}, x_{n-1},\\
&= \sum_{i=1}^{n-1}x_i,\ n=1,2,3,\ldots
\end{aligned}$$

And we assume that $x_0\in B_r(x)$, where $B_r(x)=\{x\in X:\|x'-x\|<r\}$; then, we have as follows:

(i) $x_n\in B_r(x)$

(ii) $\lim_{n\to\infty}x_n=x$

Proof
For condition (i), invoking mathematical induction,
For n=1, we have as follows:

$$\|x_0-x\|=\|T(x_0)-T(x)\|\le\|x_0-x\|.$$

If this is true for m-1, then

$$\|x_0 - x\| \le k^{m-1}\|x_0 - x\|.$$

This gives the following:

$$\|x_m - x\| = \|T(x_{m-1}) - T(x)\| \le k\|x_{m-1} - x\| \le k^n\|x_0 - x\|.$$

Therefore,

$$\|x_m - x\| \le k^n\|x_0 - x\| \le k^n r < r.$$

This directly implies that $x_n \in B_r(x)$.

Also, for (ii), we have that since $\|x_m - x\| \le k^n\|x_0 - x\|$ and $\lim_{n\to\infty} k^n = 0$, we can write $\lim_{n\to\infty} x_n = x$.

Numerical Solution of Laplace Adomian Decomposition Method (LADM)

In this section, we present the numerical solution of the model. By applying the initial conditions, the Laplace Adomian Decomposition Method (LADM) provides an approximate solution expressed as an infinite series given by:

$$\left.\begin{aligned}
S_H(t) &= 100000000 - 409.97\frac{t^\beta}{\Gamma(\beta+1)} - 815.16\frac{t^{2\beta}}{\Gamma(2\beta+1)} + \ldots\\
E_M(t) &= 25000000 - 25180.46\frac{t^\beta}{\Gamma(\beta+1)} + 5345.67\frac{t^{2\beta}}{\Gamma(2\beta+1)} + \ldots\\
I_M(t) &= 68000000 - 506.29\frac{t^\beta}{\Gamma(\beta+1)} - 75673890800\frac{t^{2\beta}}{\Gamma(2\beta+1)} + \ldots..\\
T_M(t) &= 3000000 + 6009.78\frac{t^\beta}{\Gamma(\beta+1)} + 789.06\frac{t^{2\beta}}{\Gamma(2\beta+1)} + \ldots..\\
R(t) &= 6000000 + 1400.78\frac{t^\beta}{\Gamma(\beta+1)} + 357.06\frac{t^{2\beta}}{\Gamma(2\beta+1)} + \ldots\\
S_V(t) &= 10000 + 1534.78\frac{t^\beta}{\Gamma(\beta+1)} + 648.06\frac{t^{2\beta}}{\Gamma(2\beta+1)} + \ldots\\
E_V(t) &= 6000 + 1555.78\frac{t^\beta}{\Gamma(\beta+1)} + 457.06\frac{t^{2\beta}}{\Gamma(2\beta+1)} + \ldots\\
I_V(t) &= 4500 + 1789.78\frac{t^\beta}{\Gamma(\beta+1)} + 357.06\frac{t^{2\beta}}{\Gamma(2\beta+1)} + \ldots
\end{aligned}\right\} \quad (21)$$

For $\beta = 1$, the series solution of our model becomes,

$$\left.\begin{aligned}
S_H(t) &= 100000000 - 409.97t - 407.58t^2 + \ldots\\
E_M(t) &= 25000000 - 25180.46t + 2672.835t^2 + \ldots\\
I_M(t) &= 68000000 - 506.29t - 37836945400t^2 + \ldots\\
T_M(t) &= 3000000 + 6009.78t + 394.53t^2 + ..\\
R(t) &= 6000000 + 1400.78t + 178.53t^2 + \ldots\\
S_V(t) &= 10000 + 1534.78t + 324.03t^2 + \ldots\\
E_V(t) &= 6000 + 1555.78t + 228.53t^2 + \ldots\\
I_V(t) &= 4500 + 1789.78t + 178.53t^2 + \ldots
\end{aligned}\right\} \quad (22)$$

Sensitivity Analysis of the Malaria Model

The sensitivity index of $\mathcal{R}_{0M}$ with respect to a parameter p is given by:

$$\Im_p^{R_{0M}} = \frac{p}{R_{0M}} \cdot \frac{\partial R_{0M}}{\partial p}$$

Given that:

$$\mathcal{R}_{0M} = \sqrt{\frac{(1-\phi)m^2\beta_M\beta_V\theta_M\theta_V\mu_H^2}{\Lambda_H^2(\theta_M+\mu_H)(\gamma_M+\delta_M+\mu_H)(\theta_V+\mu_V)(\delta_V+\mu_V)}}$$

Here are the simplified final sensitivity indices for the key parameters:

Sensitivity to β_M and β_V:

$$\Im_{\beta_M} = \Im_{\beta_V} = \frac{1}{2}$$

Sensitivity to θ_M:

$$\Im_{\theta_M} = \frac{1}{2} - \frac{\mu_H}{2(\theta_M+\mu_H)}$$

Sensitivity to θ_V:

$$\Im_{\theta_V} = \frac{1}{2} - \frac{\mu_V}{2(\theta_V+\mu_V)}$$

4. Sensitivity to μ_H:

$$\Im_{\mu_H} = 1 - \frac{\theta_M}{2(\theta_M+\mu_H)} - \frac{\gamma_M+\delta_M}{2(\gamma_M+\delta_M+\mu_H)}$$

5. Sensitivity to μ_V:

$$\Im_{\mu_V} = -\frac{\theta_V}{2(\theta_V+\mu_V)} - \frac{\delta_V}{2(\delta_V+\mu_V)}$$

6. Sensitivity to ϕ:

$$\Im_{\phi} = -\frac{1}{2(1-\phi)}$$

7. Sensitivity to m:

$$\Im_{m} = 1$$

8. Sensitivity to γ_M:

$$\Im_{\gamma_M} = -\frac{1}{2(\gamma_M + \delta_M + \mu_H)}$$

9. Sensitivity to δ_M and δ_V:

$$\Im_{\delta_M} = -\frac{1}{2(\gamma_M + \delta_M + \mu_H)}$$

$$\Im_{\delta_V} = -\frac{1}{2(\delta_V + \mu_V)}$$

By substituting the parameter values in table 2 into the sensitivity analysis, we obtain;

1. Sensitivity to β_M and β_V: 0.5

2. Sensitivity to θ_M: 0.3036

3. Sensitivity to θ_V: 0.4994

4. Sensitivity to μ_H: -0.6687

5. Sensitivity to μ_V: -0.3899

6. Sensitivity to ϕ: -0.0408

7. Sensitivity to m: 1

8. Sensitivity to γ_M: -2.5381

9. Sensitivity to δ_M: -2.5466

Sensitivity to δ_V: -2.2616

RESULTS AND DISCUSSION

From the sensitivity analysis above, we observed that parameters like $\beta_M, \beta_V, \theta_M, \theta_V, m$ with positivity sensitivity indices enhance the spread of malaria within the human population. Conversely, parameters like $\mu_H, \mu_V, \gamma_M, \gamma_V$ with negative sensitivity indices reduce the prevalence of malaria within the human population.

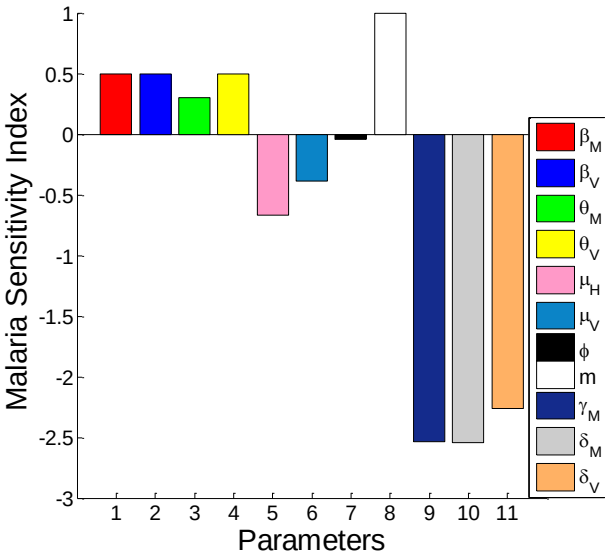

Figure 3: Sensitivity analysis bar chart for the Malaria only sub-model

The figure 3 above shows a bar chart illustrating the results of a sensitivity analysis for the malaria-model. Sensitivity analysis helps identify key parameters that influence the spread and prevalence of malaria within human populations (Haile *et al,* 2025: Adeniyi *et al*.,2024). Parameters with **positive sensitivity indices** enhance malaria transmission, meaning that an increase in their values leads to a higher spread of the disease. These may include factors like the mosquito biting rate, transmission probability, mosquito population, and the duration of infection in humans. Conversely, parameters with **negative sensitivity indices** reduce malaria prevalence, meaning that increasing these values helps control the disease. Such parameters could include the recovery rate of infected individuals, mosquito mortality rate, and the effectiveness of control measures like insecticide-treated nets (ITNs) or vaccination (Agbata *et al,* 2025). Understanding these relationships is crucial for developing targeted interventions, as reducing parameters with positive indices or increasing those with negative indices can effectively mitigate malaria transmission and prevalence.

Table 2: Parameters Table of Values

Parameter	Values	Sources
Λ_H	0.00021	(Bolarinwa *et al,* 2023)
β_M	1.000000	Fitted
K_M	0.03	(Alzahrani, and Khan, 2022)
θ_M	0.702503	Fitted

μ_H	0.0002	(Agbata *et al* , 2023)
μ_V	0.0002	(Odeh *et al*, 2024)
γ_M	0.240461	Fitted
δ_M	0.010000	Fitted,
α_M	0.064398	Fitted
ω_M	0.702503	Fitted
Λ_V	0.071	(Omeje *et al*, 2024)
β_V	0.450000	Fitted
θ_V	0.022662	Fitted
δ_V	0.039417	Fitted
ϕ	0.3	(Omeje *et al*, 2024)

Data Fitting For the Malaria model

To ensure consistency between the collected data and the mathematical sub-models for malaria and tuberculosis, the *fmincon* function from MATLAB's Optimization Toolbox was employed. This approach improves the precision of parameter estimation by optimizing the model fitting process, thereby enabling a more accurate representation of actual disease dynamics. Through this optimization, critical parameters are adjusted to minimize the gap between model outputs and observed data. The resulting fitted data plots from this procedure are shown in the figures below.

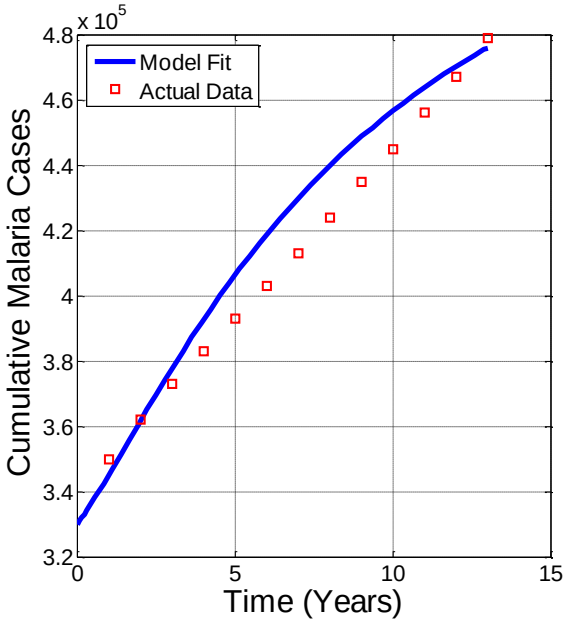

Figure 2a. Cumulative Malaria Cases.

Fitted Parameters:

$\beta_M = 1.000000$

$\beta_V = 0.450000$

$\theta_M = 0.702503$

$\theta_V = 0.022662$

$\gamma_M = 0.240461$

$\alpha_M = 0.064398$

$\omega_M = 0.600000$

$\delta_M = 0.010000$

$\delta_V = 0.039417$

$m = 0.800000$

We utilized disease infection data from Nigeria to fit our malaria and tuberculosis sub-models. For malaria, the annual data spans the years 2014 to 2021, with confirmed malaria cases provided in the Table below. Similarly, tuberculosis data was collected annually from 2010 to 2022, with confirmed cases summarized in the Table below

Malaria Data

Table 1 presents the reported malaria cases from 2010 to 2022 in Nigeria. These figures were sourced from the **World Health Organization (WHO).**

Year	**Cases**
2010	350,000
2011	362,000
2012	373,000
2013	383,000
2014	393,000
2015	403,000
2016	413,000
2017	424,000
2018	435,000

2019	445,000
2020	456,000
2021	467,000
2022	479,000

Source: (WHO, 2023)

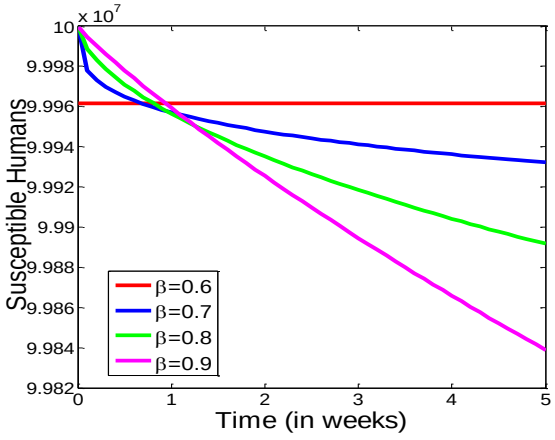

Figure 3a. Effect of varying β on susceptible human population

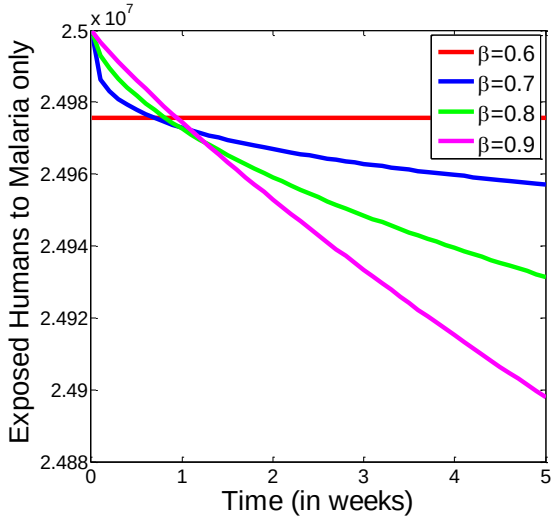

Figure 3b. Effect of varying β on exposed humans to malaria population

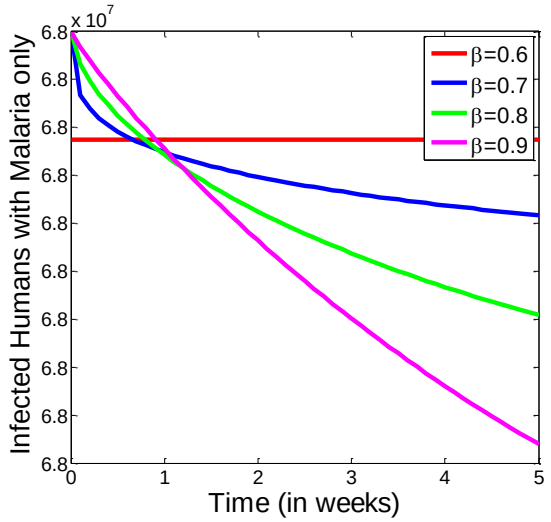

Figure 3c. Effect of varying β on humans Infected with malaria

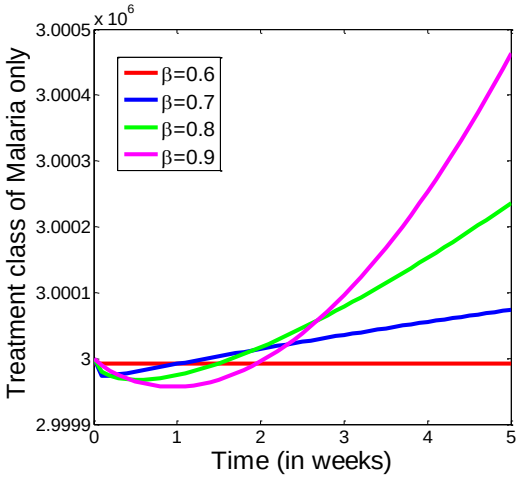

Figure 3d. Effect of varying β on treatment class humans infected with malaria

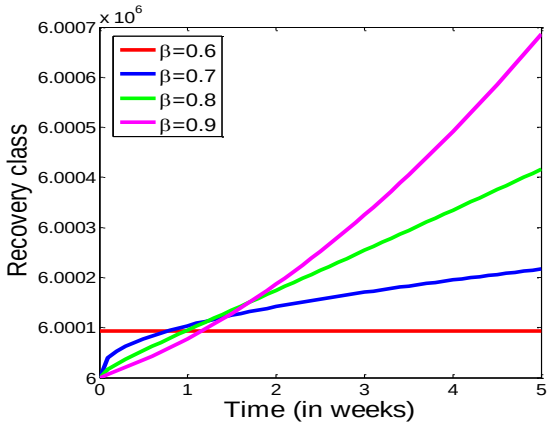

Figure 3e. Effect of varying β on recovered Humans

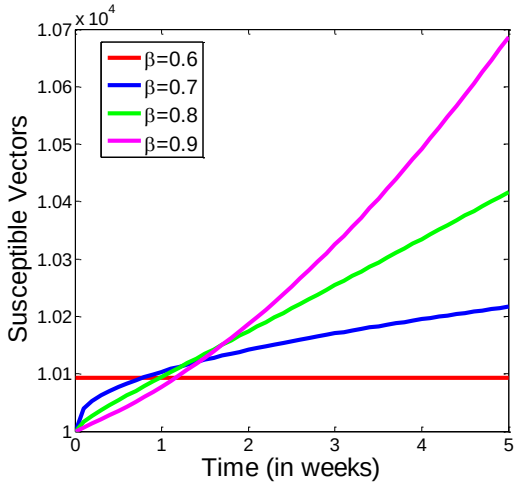

Figure 3f. Effect of varying β on susceptible vectors

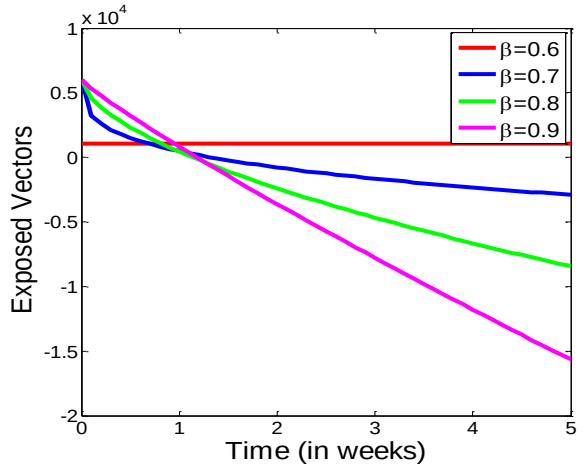

Figure 3g. Effect of varying β on exposed vector population

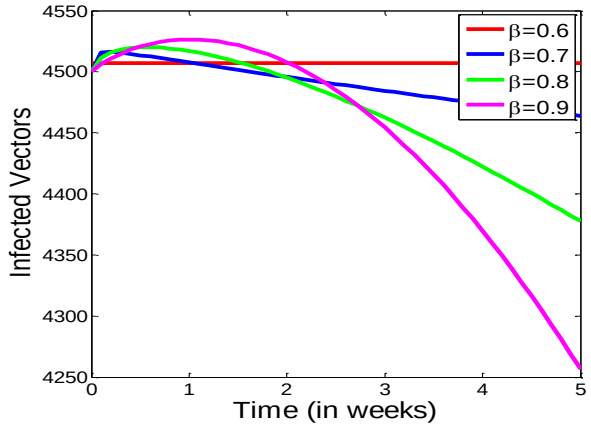

Figure 3h. Effect of varying β on infected vectors

In **Figure 3a**, as the contact rate increases, the population of susceptible individuals declines over time. This suggests that malaria spreads more rapidly when there is more interaction between susceptible and infected individuals. However, it also indicates that implementing effective control measures—such as reducing human-vector contact—can significantly curb the disease's spread. Similarly, in **Figure 3b**, the number of exposed humans decreases over time as the contact rate increases. This trend suggests that when proper interventions are in place, fewer individuals progress from the susceptible to the exposed stage of infection. **Figure 3c** shows a decline in the number of infected humans as the contact rate rises. One possible explanation for this is the implementation of high treatment coverage, as observed in **Figure 3d**, where effective medical interventions contribute to a higher recovery rate. This is further supported by **Figure 3e**, which shows a significant increase in the number of recovered individuals due to timely and effective treatment. Regarding the mosquito population, **Figure 3f** indicates an increase in the number of susceptible vectors as the contact rate increases. This could mean that fewer mosquitoes become infected, possibly due to reduced human-to-vector transmission. Meanwhile, **Figure 3g** shows a decrease in the number of exposed vectors over time, reinforcing the idea that transmission is being disrupted. In **Figure 3h**, the number of infected vectors declines, which can be attributed to the success of control measures such as insecticide use, environmental management, and reduced human-vector interaction. The findings highlight that malaria transmission can be significantly reduced—and potentially eradicated when appropriate control measures are implemented. Reducing contact rates between humans and infected vectors through behavioral changes and protective measures plays a crucial role in slowing the spread of the disease. Encouraging prompt and effective treatment ensures that infected individuals recover faster, thereby reducing the number of infectious hosts in the population. Additionally, strong vector control strategies, such as the use of insecticides, mosquito nets, and environmental modifications to eliminate breeding sites, further disrupt transmission. When these measures are effectively combined and sustained, the burden of malaria can be greatly minimized, ultimately leading to its eradication from the population.

CONCLUSION

This study applied sensitivity analysis and the Laplace-Adomian Decomposition Method (LADM) to analyze a fractional-order malaria transmission model. By developing a deterministic compartmental model, we identified key factors influencing disease spread and evaluated the impact of various control strategies. Our

analysis demonstrated that malaria transmission is significantly influenced by contact rates between susceptible humans and infected vectors, as well as the effectiveness of treatment within the human population. The results from our numerical simulations indicate that increasing the contact rate leads to a decline in the susceptible human population, reinforcing the importance of minimizing human-vector interactions. Moreover, the reduction in the number of exposed and infected individuals, as seen in our model, highlights the effectiveness of early treatment interventions. The findings also suggest that implementing timely and effective medical treatments enhances recovery rates, ultimately reducing the pool of infectious individuals and disrupting disease transmission.

In terms of vector dynamics, our results show that reducing human-to-vector transmission leads to fewer infected mosquitoes, which further limits the spread of malaria. Control strategies such as insecticide-treated bed nets, environmental management, and mosquito population control prove to be critical in minimizing the number of infectious vectors in the population. The study demonstrates the importance of integrating multiple intervention strategies to effectively combat malaria. Reducing human-vector contact through protective measures, ensuring prompt treatment of infected individuals, and implementing robust vector control methods are essential in minimizing malaria prevalence. The use of fractional-order models in disease dynamics, particularly with the application of LADM, provides a more comprehensive and accurate representation of malaria transmission, offering valuable insights for disease control and eradication efforts.

Data Availability

All the data used in the study of this research work have been adequately cited.

Conflicts of Interest

The authors declare that they have no conflict of interest.

REFERENCE

Acheneje, G. O., Omale, D., Agbata, B. C., Atokolo, W., Shior, M. M., and Bolawarinwa, B. (2024). Approximate solution of the fractional order mathematical model on the transmission dynamics of the co-infection of COVID-19 and Monkeypox using Laplace-Adomian Decomposition method. *IJMSS, 12*(3), 17–51.

Adeniyi, M. O., Amalare, A. A., Oke, S. I., and Salawu, S. O. (2024). Bifurcation analysis and global sensitivity index for malaria disease transmission dynamics: Information and treated bed nets control. *International Journal of Biomathematics, 17*(06), 2350060.

Agbata, B. C., Raimonda D, Asante Mensa, F., Kwabi, P. A., Odeh J.O., Amoah-Mensah, J., Meseda P.K and Obeng-Denteh, W.,(2025) Mathematical modelling of measles disease with double dose vaccination. *Journal of Basic and Applied Sciences Research 3*(3), 199–214. https://doi.org/10.4314/jobar.v3i3.22.

Agbata, B. C., Agbebaku, D. F., Odo, C. E., Ojih, J. T., Shior, M. M., and Ezugorie, I. G. (2024). A mathematical model for the transmission dynamics of COVID-19 in Nigeria and its post-effects. *International Journal of Mathematical Analysis and Modelling, 7*(2), 523–547. https://tnsmb.org/journal/index.php/ijmam/article/view/191

Agbata, B. C., Obeng-Denteh, W., Agbebaku, D. F., Shior, M. M., Yahaya, D. J., and Danjuma, A. Y. (2024). Laplace-Adomian Decomposition Method for solving fractional-order mathematical model of monkeypox transmission dynamics. *International Journal of Mathematical Analysis and Modelling, 7*(2), 558–588. https://tnsmb.org/journal/index.php/ijmam/article/view/193

Agbata, B. C., Obeng-Denteh, W., Amoah-Mensah, J., Kwabi, P. A., Shior, M. M., Asante Mensa, F., and Abraham, S. (2024). Numerical solution of fractional order model of measles disease with double dose vaccination. *DUJOPAS, 10*(3b), 202–217.

Agbata, B. C., Obeng-Denteh, W., Dervishi, R., Kwabi, P. A., Aal-Rkhais, H. A., Asente-Mensa, F., Ezugorie, I. G., and Arivi, S. S. (2024). Mathematical modeling and analysis of monkeypox transmission dynamics with treatment and quarantine interventions. *Dutse Journal of Pure and Applied Sciences (DUJOPAS), 10*(4b), 78–96. https://www.ajol.info/index.php/dujopas/article/view/264210

Alzahrani, A. K., and Khan, M. A. (2022). The co-dynamics of malaria and tuberculosis with optimal control strategies. *Filomat, 36*(6), 1789–1818. https://doi.org/10.2298/FIL2206789A

Ashley, E. A., Dhorda, M., Fairhurst, R. M., Amaratunga, C., Lim, P., Suon, S., and Dondorp, A. M. (2023). Spread of artemisinin resistance in *Plasmodium falciparum*

malaria. *The New England Journal of Medicine, 389*(10), 947–958.

Bhattacharya, S., Sharma, R., and Singh, M. (2023). *Plasmodium* and *Mycobacterium tuberculosis*: Immunological interplay and co-infection outcomes. *Clinical Infectious Diseases, 75*(1), 77–86. https://doi.org/10.1093/cid/ciad357

Bhatt, S., Weiss, D. J., Cameron, E., Bisanzio, D., Mappin, B., Dalrymple, U., and Gething, P. W. (2022). The effect of malaria control on *Plasmodium falciparum* in Africa between 2000 and 2015. *Nature, 526*(7572), 207–211.

Bolarinwa, B., Thomas Onoja, Agbata, B. C., Omede, B. I., and Odionyenma, U. B. (2024). Dynamical analysis of HIV-TB coinfection in the presence of treatment for TB. *Bulletin of Biomathematics, 2*(1), 21–56.

Cator, L. J., Benedict, M. Q., and Reddy, M. R. (2023). Environmental determinants of malaria transmission in East Africa: Climate, vectors, and parasites. *International Journal of Parasitology, 53*(4), 311–324. https://doi.org/10.1016/j.ijpara.2023.04.005

Chitnis, N., Hyman, J. M., and Cushing, J. M. (2008). Determining important parameters in the spread of malaria through the sensitivity analysis of a mathematical model. *Bulletin of Mathematical Biology, 70*(5), 1272–1296.

Diethelm, K. (2022). *The analysis of fractional differential equations: An application-oriented exposition using differential operators of Caputo type*. Springer Science and Business Media.

Draper, S. J., Sack, B. K., King, C. R., Nielsen, C. M., Rayner, J. C., and Higgins, M. K. (2022). Malaria vaccines: Recent advances and new horizons. *Cell Host and Microbe, 30*(2), 161–177.

Ghosh, S., Banerjee, S., and Chakraborty, P. (2022). Multidrug-resistant tuberculosis and its global implications: Current strategies for detection and treatment. *Global Health Action, 15*(1), 204–213. https://doi.org/10.1080/16549716.2022.2054132

Haile, G. T., Koya, P. R., and Mosisa Legesse, F. (2025). Sensitivity analysis of a mathematical model for malaria transmission accounting for infected ignorant humans and relapse dynamics. *Frontiers in Applied Mathematics and Statistics, 10*, 1487291.

Hemingway, J., Shretta, R., Wells, T. N., Bell, D., Djimde, A. A., Achee, N., and Qi, G. (2022). Tools and strategies for malaria control and elimination: What do we need to achieve a grand convergence in malaria? *PLoS Biology, 14*(3), e1002380.

Ndii, M., Tong, S. Y., Andrews, R. M., McVernon, J., and Riley, T. V. (2020). Sensitivity analysis of a mathematical model of *Plasmodium falciparum* malaria transmission. *Mathematical Biosciences, 322*, 108292.

Ngonghala, C. N., Del Valle, S. Y., Zhao, R., Mohammed-Awel, J., and Gumel, A. B. (2021). Quantifying the impact of human mobility on malaria dynamics and control. *Journal of Theoretical Biology, 505*, 110398.

Odeh, J. O., Agbata, B. C., Ezeafulukwe, A. U., Madubueze, C. E., Acheneje, G. O., and Topman, N. N. (2024). A mathematical model for the control of chlamydia disease with treatment strategy. *Journal of Mathematical Analysis and Research, 7*(1), 1–20.

Olumuyiwa, J. P., Sumit, K., Nitu, K., Festus, A. O., Kayode, O., and Rabiu, M. (2022). Transmission dynamics of monkeypox virus: A mathematical modeling approach. *Modeling Earth System and Environment*. https://doi.org/10.1007/s40808-021-013313-2

Omeje, D., Acheneje, G., Odiba, P., and Bolarinwa, B. (2024). Modelling the transmission dynamics of the coinfection of malaria and tuberculosis with optimal control strategies cost effectiveness analysis. *Research Square*. Preprint. https://doi.org/10.21203/rs.3rs-5312505/v1

Pamungkas, Y., and Eljatin, D. S. (2024). Hyperparameter tuning of EfficientNet method for optimization of malaria detection system based on red blood cell image. *Jurnal Sisfokom (Sistem Informasi dan Komputer), 13*(3), 360–368.

Parham, P. E., and Michael, E. (2022). Modeling the effects of weather and climate change on malaria transmission. *Environmental Health Perspectives, 118*(5), 620–626.

Reiner, R. C., Geary, M., Atkinson, P. M., Smith, D. L., and Tatem, A. J. (2023). A systematic review of mathematical models of mosquito-borne pathogen transmission: 2000–2020. *Epidemics, 41*, 100547.

Ryan, S. J., Carlson, C. J., Mordecai, E. A., and Johnson, L. R. (2023). Global expansion and redistribution of

Aedes mosquitoes due to climate change. *Nature Communications, 14*(1), 1–10.

World Health Organization. (2023). *World malaria report 2023*. https://www.who.int/publications/i/item/9789240068487